Journal of Solid State Chemistry 182 (2009) 1129–1135

Contents lists available at ScienceDirect

Journal of Solid State Chemistry

journal homepage: www.elsevier.com/locate/jssc

Barium aluminides Ba_xAl_5 ($x = 3, 3.5, 4$)

Michael Jehle, Harald Scherer, Marco Wendorff, Caroline Röhr *

Institut für Anorganische und Analytische Chemie, University of Freiburg, Germany, Albertstr. 21, D-79104 Freiburg, Germany

ARTICLE INFO

Article history:
Received 24 November 2008
Received in revised form
16 January 2009
Accepted 1 February 2009
Available online 21 February 2009

PACS:
61.66.Fn
71.20.Lp

Keywords:
Aluminides
Crystal structure
Band structure calculation
Al MAS-NMR spectroscopy

ABSTRACT

Three aluminides of the series Ba_xAl_5 ($x = 3, 3.5, 4$) were synthesized from stoichiometric ratios of the elements in Ta crucibles. The crystal structure of the new compound Ba_7Al_{10} was determined using single crystal X-ray data (space group $R\bar{3}m$, $a = 604.23(9)$, $c = 4879.0(12)$ pm, $Z = 3$, $R1 = 0.0325$). The compound exhibits Al Kagomé (3.6.3.6.) nets in which half of the triangles form the basis of trigonal bipyramids Al_5. The apical Al are thus three-bonded assuming a charge of -2 (^{27}Al-NMR chemical shift $\delta = 660$ pm), whereas the Al atoms of the basal triangle (i.e. of the Kagomé net) are four-bonded and thus of formal charge -1 ($\delta = 490$ ppm). The total charge of the anion is thus exactly compensated by the Ba cations, i.e. the compound can be interpreted as an electron precise *Zintl* phase, exhibiting a distinct pseudo-band gap at the Fermi level of the calculated tDOS. According to the total formula, the structure displays a combination the stacking sequences of Ba_3Al_5 and Ba_4Al_5, the structures of which have been redetermined with current methods (both hexagonal with space group $P6_3/mmc$; Ba_3Al_5: $a = 606.55(7)$, $c = 1461.8(2)$ pm, $Z = 2$, $R1 = 0.0239$; Ba_4Al_5: $a = 609.21(7)$, $c = 1775.8(3)$ pm, $Z = 2$, $R1 = 0.0300$). These three compounds with slightly different electron counts but similar polyanions allow to compare the bond lengths, the electronic structures and the overall bonding situation in dependence of positive or negative deviation of the electron count in relation to the novel formally electron precise *Zintl* compound Ba_7Al_{10}.

1. Introduction

Binary trielides (M^{III}) of the alkaline earth elements (A^{II}) are interesting phases to investigate the validity of simple electron counting rules such as the *Zintl* concept and the *Wade* rules. Compared to the gallides and indides, where electron precise *Zintl* compounds are common [1–3], the corresponding aluminides, i.e. the compounds with the less electronegative triel element, often exhibit the structural features of the *Laves* phases, such as *M* Kagomé nets (3.6.3.6. nets after *Schläfli*). $CaAl_2$ [4] for instance crystallizes with the $MgCu_2$ structure type and most of the binary Ba aluminides in the composition range of 1:1–1:2 (ratio Ba:Al) also exhibit Kagomé nets as predominating structural units [5–7]: Ba_7Al_{13} [7] the composition of which has been recently corrected to $Ba_{21}Al_{40}$ [8] exhibits blocks of three Kagomé nets as a section of the $MgCu_2$ structure. Blocks of two connected Kagomé nets are present in the structure of Sr_5Al_9 [9] and in several ternary mixed trielides [10]. In the more Ba-rich compounds Ba_3Al_5 [5] and Ba_4Al_5 [6] single Al Kagomé nets are fully separated by the Ba counter ions. Despite the different electron count, the latter two compounds contain nearly identical Al polyanions. A formal analysis of this polyanion from the *Zintl* point of view shows that due to two three-(Al^{2-}) and three four-bonded (Al^{-}) Al atoms the polyanion should bear a charge of minus 7 ($[Al_2Al_3]^{7-}$) which means that the number of counter cations is too small in Ba_3Al_5 [11] and too large in Ba_4Al_5. The two compounds thus call for a detailed study of the electronically driven geometrical and bonding changes, which might be explained using the results of bandstructure calculations. Due to the risk of hydride impurities especially in Ba-rich compounds and the fact, that the structural data are those of 1975 (in the case of Ba_4Al_5 refined from film data) both compounds were newly prepared and the structures were refined using X-ray diffractometer data. Possible hydrogen impurities can be ruled out on the basis of these measurements. In addition, the absence of hydrogen was confirmed using MAS-NMR spectroscopy. Surprisingly, in the course of the corresponding synthetic work, the preparation and structural characterization of the exactly electron precise intermediate phase $Ba_{3.5}Al_5$ has been achieved, so that we are now able to analyse the whole series of compounds Ba_xAl_5 with $x = 3$, 3.5 and 4, which all exhibit identical Al Kagomé nets.

2. Experimental section

2.1. Preparation

The synthesis of the title compounds was generally performed starting from the elements barium and aluminium obtained from

* Corresponding author.
E-mail address: caroline@ruby.chemie.uni-freiburg.de (C. Röhr).

0022-4596/$ - see front matter © 2008 Elsevier Inc. All rights reserved.
doi:10.1016/j.jssc.2009.02.005

commercial sources and used without further purification (Ba: Metallhandelsgesellschaft Maassen, Bonn, 99% and Al: ABCR Karlsruhe, 99.9%). The educts were filled into tantalum crucibles under an argon atmosphere and the sealed containers were heated up to maximum temperatures of 1075–1175 K with a constant heating rate of 200 K/h; 20 K/h was used as cooling rate. Representative parts of the reguli were ground and sealed in capillaries with a diameter of 0.3 mm. X-ray powder diagrams were collected on transmission powder diffraction systems (STADI P, linear PSD, Fa. Stoe Cie, Darmstadt, Mo$K\alpha$ radiation, graphite monochromator).

The preparation of phase pure samples turned out to be rather difficult as the compositions of the three phases are quite similar (Ba:Al ratios of 0.6, 0.7 and 0.8) and their melting behaviour is unknown. Samples with a 3:5 ratio of the elements barium and aluminium lead to powder diffractograms that contained peaks assignable to the Ba-poor compound $Ba_{21}Al_{40}$ [8] (formerly known as Ba_7Al_{13} [7]). Samples with an increased Ba proportion (e.g. Ba_4Al_5 or BaAl) finally yielded two of the three title compounds. Finally, very Ba-rich starting compositions (e.g. Ba_3Al: 939.4 mg (6.841 mmol) Ba; 63.0 (2.335 mmol) Al) yielded Ba_4Al_5 as the only aluminide product, but this is accompanied by a considerable excess of elemental barium. Due to these circumstances, an X-ray powder verification of the phase composition and the NMR spectroscopic analysis of this sample were not possible. For the MAS-NMR experiments (see below) a sample of the starting stoichiometry Ba_3Al_2 (884.2.4 mg (6.439 mmol) Ba; 116.2 (4.307 mmol) Al) was used, which according to the powder X-ray pattern consists of both compounds Ba_3Al_5 and $Ba_{3.5}Al_5$. The single crystals of all three title compounds form to some extent well developed plates, show silvery metallic lustre and are sensitive against air and moisture.

2.2. Crystal structure determination

For the crystal structure determinations, single crystals were selected using a stereo microscope and mounted in glass capillaries (diameter 0.1 mm) under dried paraffine oil. The crystals were centered on a diffractometer equipped with an image plate detector.

The diffraction data of Ba_3Al_5 and Ba_4Al_5 both showed a hexagonal lattice with a high Laue class symmetry and the additional systematic absence conditions reflections *hhl* only present for $l = 2n$. The possible space groups $P6_3mc$ and $P6_3/mmc$, and the lattice constants both agreed with the structural models of Ba_3Al_5 and Ba_4Al_5 reported by *Fornasini* in 1975 [5,6]. The least squares refinement of the corresponding atomic coordinates applying anisotropic thermal parameters for all atom positions (program SHELXL-97 [12]) converged at low residual values of 0.024 and 0.030. The residual difference electron density maxima of approx. 2 e/pm^3 are all located in the vicinity of the Ba atoms, potential hybrid positions (as were nicely seen in the structure analysis of the indide hydride Ba_9In_4H [13]) are not present at all. In the case of the Ba-rich compound Ba_4Al_5, which had been formerly refined using film data only, the reported problem of an

Table 2
Atomic coordinates and equivalent isotropic displacement parameters (pm^2) in Ba_3Al_5 (above), $Ba_{3.5}Al_5$ (middle) and Ba_4Al_5 (below).

Atom	Wyckoff position	x	y	z	$U_{equiv.}$
Ba(1)	4*f*	$\frac{1}{3}$	$\frac{2}{3}$	0.62512(3)	149(2)
Ba(2)	2*a*	0	0	0	289(2)
Al(1)	4*f*	$\frac{1}{3}$	$\frac{2}{3}$	0.1140(2)	242(6)
Al(2)	6*h*	0.1549(2)	2*x*	$\frac{1}{4}$	228(4)
Ba(1)	6*c*	0	0	0.129079(16)	186(2)
Ba(2)	6*c*	0	0	0.052129(16)	203(2)
Ba(3)	3*b*	0	0	$\frac{1}{2}$	320(3)
Ba(4)	6*c*	0	0	0.359336(18)	238(3)
Al(11)	6*c*	0	0	0.28409(9)	218(9)
Al(12)	6*c*	0	0	0.20094(8)	193(8)
Al(2)	18*h*	0.4907(2)	0.5093(2)	0.09121(4)	198(5)
Ba(1)	4*f*	$\frac{1}{3}$	$\frac{2}{3}$	0.56944(4)	195(2)
Ba(2)	4*e*	0	0	0.14214(4)	159(2)
Al(1)	4*f*	$\frac{1}{3}$	$\frac{2}{3}$	0.1362(2)	172(7)
Al(2)	6*h*	0.5102(3)	2*x*	$\frac{1}{4}$	150(5)

Table 1
Crystallographic data, details of the data collection and structural determination for the title compounds Ba_xAl_5 ($x = 3, 3.5, 4$).

x in Ba_xAl_5		3	3.5	4
Crystal system		Hexagonal	Trigonal	Hexagonal
Space group		$P6_3/mmc$	$R\bar{3}m$	$P6_3/mmc$
		No. 194	No. 166	No. 194
Lattice constants (pm)	*a*	606.55(7)	604.23(9)	609.21(7)
	c	1461.8(2)	4879.0(12)	1775.8(3)
Volume of the u.c. (10^6 pm^3)		465.7(1)	1542.7(5)	570.8(1)
Z		2	3 (6)	2
Density (X-ray) (g/cm^3)		3.90	3.98	3.98
Diffractometer		Stoe IPDS-2		
Absorption coeff. $\mu_{MoK\alpha}$ (mm^{-1})		12.92	13.58	13.93
θ range (deg)		2.8–28.1	2.5–29.2	2.3–29.1
No. of reflections collected		5579	4971	7869
No. of independent reflections		277	601	343
R_{int}		0.1161	0.0671	0.0634
Corrections		Lorentz, Polarization, Absorption		
Structure solution		SHELXS-97 [14]		
Refinement		SHELXL-97 [12]		
No. of free parameters		13	25	15
Goodness-of-fit on F^2		1.132	1.007	1.131
R values (for refl. with $I \geq 2\sigma(I)$)	*R*1	0.0239	0.0325	0.0300
	*wR*2	0.0585	0.0769	0.0621
R values (all data)	*R*1	0.0271	0.0423	0.0391
	*wR*2	0.0593	0.0792	0.0643
Residual elect. density (e$^-$ × 10^{-6} pm^{-3})		+1.1/−2.1	+1.6/−1.3	+2.3/−1.1

unphysically large isotropic displacement parameter of one Al position was resolved due to the much better quality and completeness of the new data set.

The reflections of the intermediate aluminide $Ba_{3.5}Al_5$ could be indexed using a rhombohedral lattice with a very similar hexagonal basis, but a quite large *c* lattice parameter of nearly 5 nm. The high Laue symmetry and the lack of further absence conditions indicated the possible space groups $R\bar{3}m$ and $R3m$. The structure was solved by direct methods (program SHELXS-97 [14]) in the centrosymmetric space group. This structure solution yielded the four Ba positions. The three Al positions were found by a successive refinement and a difference electron density synthesis. The final least squares refinement of the atomic coordinates applying anisotropic thermal parameters for all sites resulted in a similarly low *R*1 value of 0.0325.

The crystallographic data and the refined atomic parameters are summarized in the Tables 1 and 2, respectively. Selected interatomic distances are collected in Table 3 [15].

2.3. MAS-NMR spectroscopy

^{27}Al magic angle spinning nuclear magnetic resonance experiments were performed on a Bruker Avance II WB 400 MHz spectrometer ($B_0 = 11.74$ T) with a 4 mm CP-MAS probe head. The powdered sample of a mixture of Ba_3Al_5 and Ba_7Al_{10} was sealed under an argon atmosphere in a KelF inlay, which in turn was tightly fitting into a 4 mm zirconia rotor. For ^{27}Al-NMR, one pulse experiments were carried out with varying sample spinning rates between 0 and 15 kHz. Spectra were detected with a relaxation delay of 0.1 s and an acquisition time of 0.02 s. The two compounds with similar polyanions both contain two crystallographically independent aluminium atoms in a two to three ratio, which gives rise to two peaks at chemical shifts of 660 and 490 ppm with respect to a 1.1 M solution of $Al(NO_3)_3$ in D_2O. The integral of the two maxima clearly allows to assign the 660 pm signal to the three-bonded Al^{2-} atoms (2×) and the 490 ppm signal to the four-bonded Al^{-} atoms (3×). ^{1}H-NMR

Table 3
Selected interatomic distances (pm) in Ba_3Al_5 (above), $Ba_{3.5}Al_5$ (middle) and Ba_4Al_5 (below).

Atoms	Distance	Bo.	Mult.	CN	Atoms	Distance	Bo.	Mult.	CN
Ba(1)–Al(1)	349.6(3)				Ba(2)–Al(1)	387.8(2)		6×	
Ba(1)–Al(1)	350.57(4)		3×		Ba(2)–Ba(1)	395.08(4)		6×	6 + 6
Ba(1)–Al(2)	354.19(4)		6×						
Ba(1)–Ba(1)	365.10(10)								
Ba(1)–Ba(2)	395.08(4)		3×	10 + 4					
Al(1)–Al(2)	273.2(3)	*a*	3×		Al(2)–Al(1)	273.2(3)	*a*	2×	
Al(1)–Ba(1)	349.6(3)				Al(2)–Al(2)	281.9(4)	*b*	2×	
Al(1)–Ba(1)	350.57(4)		3×		Al(2)–Al(2)	324.6(4)	*c*	2×	
Al(1)–Ba(2)	387.8(2)		2×	3 + 6	Al(2)–Ba(1)	354.19(4)		4×	
					Al(2)–Ba(2)	400.06(11)		2×	6 + 6
Ba(1)–Al(12)	349.23(6)		3×		Ba(2)–Al(11)	349.13(6)		3×	
Ba(1)–Al(12)	350.6(4)				Ba(2)–Al(2)	357.40(13)		6×	
Ba(1)–Al(2)	354.26(12)		6×		Ba(2)–Ba(4)	371.42(6)		3×	
Ba(1)–Ba(2)	375.4(2)				Ba(2)–Ba(1)	375.44(15)			9 + 4
Ba(1)–Ba(3)	394.11(6)		3×	10 + 4					
Ba(3)–Al(12)	386.9(2)		6×		Ba(4)–Al(2)	358.3(2)		3×	
Ba(3)–Ba(1)	394.11(6)		6×	6 + 6	Ba(4)–Al(11)	366.8(2)		3×	
					Ba(4)–Al(11)	367.1(5)			
					Ba(4)–Ba(2)	371.42(7)		3×	
					Ba(4)–Ba(4)	431.38(12)		3×	7 + 6
Al(11)–Al(2)	275.4(4)	*a*′	3×		Al(2)–Al(12)	272.6(4)	*a*″		
Al(11)–Ba(2)	349.13(6)		3×		Al(2)–Al(11)	275.4(4)	*a*′		
Al(11)–Ba(4)	366.8(2)		3×		Al(2)–Al(2)	285.2(4)	*b*	2×	
Al(11)–Ba(4)	367.2(5)			3+7	Al(2)–Al(2)	319.1(4)	*c*	2×	
					Al(2)–Ba(1)	354.26(12)		2×	
Al(12)–Al(2)	272.6(4)	*a*″	3×		Al(2)–Ba(2)	357.40(13)		2×	
Al(12)–Ba(1)	349.23(6)		3×		Al(2)–Ba(4)	358.3(2)			
Al(12)–Ba(1)	350.6(4)				Al(2)–Ba(3)	403.3(2)			6 + 6
Al(12)–Ba(3)	386.9(2)		3×	3 + 7					
Ba(1)–Al(2)	360.6(2)		3×		Ba(2)–Al(1)	351.89(4)		3×	
Ba(1)–Al(1)	365.1(4)				Ba(2)–Al(2)	359.99(5)		6×	
Ba(1)–Al(1)	371.14(13)		3×		Ba(2)–Ba(1)	374.67(5)		3×	
Ba(1)–Ba(2)	374.67(5)		3×		Ba(2)–Ba(2)	383.10(14)			9 + 4
Ba(1)–Ba(1)	429.65(9)		3×	7 + 6					
Al(1)–Al(2)	275.1(3)	*a*	3×		Al(2)–Al(1)	275.1(3)	*a*	2×	
Al(1)–Ba(2)	351.89(4)		3×		Al(2)–Al(2)	286.0(5)	*b*	2×	
Al(1)–Ba(1)	365.1(4)				Al(2)–Al(2)	323.2(5)	*c*	2×	
Al(1)–Ba(1)	371.14(13)		3×	3 + 7	Al(2)–Ba(2)	359.99(5)		4×	
					Al(2)–Ba(1)	360.6(2)		2×	6 + 6

Table 4
Details of the calculation of the electronic structures of Ba_3Al_5, $Ba_{3.5}Al_5$ and Ba_4Al_5.

		Ba_3Al_5	Ba_7Al_{10}	Ba_4Al_5
Crystal data			Tables 1 and 2	
R_{mt} (all atoms)			121.7 pm (2.3 a.u.)	
$R_{mt} \cdot K_{max}$			8.0	
k-Points/BZ		980	1000	784
k-Points/IBZ		72	110	72
Monkhorst-Pack-Grid		$14 \times 14 \times 5$	$10 \times 10 \times 10$	$14 \times 14 \times 4$
DOS			Fig. 3	
	Bond			
Electron density at BCP ($e^- \times 10^{-6}$ pm^{-3}) (*d* (pm))	*a*	0.237 (273.2)	0.233 (275.4) 0.242 (272.6)	0.234 (275.1)
	b	0.221 (281.9)	0.214 (285.2)	0.212 (286.0)
	c	−(324.6)	−(319.1)	−(323.2)
Charge distribution (after *Bader*)	Al(11)	−0.764	−0.917	−0.836
	Al(12)	–	−0.717	–
	Al(2)	−0.390	−0.420	−0.452

spectra were acquired at a spinning rate of 15 kHz with a relaxation delay of 1200 s and an acquisition time of 1.36 s, accumulating 33 scans. No signal could be detected indicating the presence of H^-. The spectrum obtained resembles a ^{1}H-MAS-NMR spectrum of a NaCl sample measured with the same set-up and under the same conditions.

2.4. Band structure calculation

For the three title compounds, DFT calculations of the electronic band structures were performed using the FP-LAPW method (program WIEN2K [16]). The exchange-correlation contribution was described by the *generalized gradient approximation* (GGA) of *Perdew*, *Burke* and *Ernzerhof* [17]. Muffin-tin radii were chosen as 121.7 pm (2.3 a.u.) for all atoms. Cutoff energies used are $E_{max}^{pot} = 14$ Ry (potential) and $E_{max}^{wf} = 12.5$ Ry (interstitial PW). Electron densities and *Fermi* surfaces were calculated and visualized using the programs XCRYSDEN [18] and DRAWXTL [19]. A *Bader* analysis of the electron density map was performed to evaluate the charge distribution between the atoms [20] and the bond critical points. Further details and selected results of the calculations are summarized in Table 4. The total and selected partial Al density of states are depicted in Fig. 3 for all three aluminides.

3. Results and discussion

3.1. Crystal structure description and comparison

As in numerous other alkaline-earth aluminides like $CaAl_2$ [3,4], the high pressure form of $SrAl_2$ [21,22] and $Ba_7Al_{13}/Ba_{21}Al_{40}$ [7,8,10] the crystal structures of all the title compounds exhibit Al Kagomé (3.6.3.6.) nets, which are stacked along the *c* axis. In contrast to the more Al-rich compounds, the layers in the title compounds are isolated from each other by the relatively large number of Ba cations. In these aluminides, one half of the $Al(2)_3$ triangles of the Kagomé nets are considerably enlarged (Al–Al distance *c*) and form the base of trigonal bipyramids $Al(2)_3Al(1X)_2$) (Fig. 1, grey box). An alternative description of the layers is in terms of connecting trigonal bipyramids, via $Al(2)_3$ triangles. The Al(1) vertices of the bipyramids are three-bonded (Al(1)–Al(2) distance *a*) and thus of formal charge −2. Neglecting the long Al(2)–Al(2) distances *c*, the Al(2) base atoms are four-bonded and can thus be expected to be Al^-. Overall, the charge/f.u. (charge/M_5) should be −7 from the *Zintl* point of view.

In the Ba-poor compound Ba_3Al_5 (Fig. 1(a)), which was already described by *Fornasini* [5], the layers are stacked in cross position according to the sequence |:AB:| along the hexagonal *c* axis. The Al–Al distance *a* from the apical Al(1) to the basal Al(2) atoms is 273.2 pm (see Table 3) and thus nicely compares to the Al–Al distances in the Al_4^{8-} tetrahedra of $Sr_{14}[Al_4]_2[Ge]_3$ (269.7–273.6 pm [23]). The bond distance Al(2)–Al(2) (distance *b*) is significantly larger (281.9 pm), but still comparable to Al^-–Al^- distances like those present in $SrAl_2$ (278.6–293.0 pm [3,24]). The third Al–Al contact (*c*), which does not show any bond critical point in the calculated electron density map (see below), is at 324.6 pm. The Ba cations next to the Kagomé net (Ba(1)) are surrounded by 10 Al and four Ba atoms, where the latter form a tetrahedral arrangement. The second Ba position in between the Al nets exhibits a 6 + 6 coordination.

In the Ba-rich compound Ba_4Al_5 (Fig. 1(c)) crystallizing with the same space group, the length of the *c* axis is increased due to the extra Ba atoms in between the Al sheets, the stacking of the Kagomé net is changed to an |:A−A′:| arrangement, where the 3.6.3.6. nets themselves are stacked in identical orientation but small and wide triangles alternate in the *c* direction. The Al–Al distances are slightly larger when compared to those in Ba_3Al_5 (*a*: 275.1 pm; *b*: 286.0 pm). The two crystallographically independent Ba cations are of the same multiplicity in this case, which means that the multiplicity of the Ba(2) site (4*e*: 0,0,*z*) is twice that of the Ba(2) site in Ba_3Al_5 (2*a*: 0,0,0). The Ba(2) cations adjacent to the Kagomé net show a very similar coordination number of 9 + 4, whereas Ba(1) is now surrounded by seven aluminium and six barium atoms (see Table 3).

The new intermediate compound Ba_7Al_{10} exactly fits the electron count expected by the *Zintl* concept (see above). According to the total formula, the stacking of the specified layers is a mixture of those observed for Ba_3Al_5 and Ba_4Al_5 (Fig. 1(b)): Stacking sequences |:AB:| (like in Ba_3Al_5) alternate with identical orientation of the Kagomé nets, resulting in an overall rhombohedral sequence |:AABBCC:|. As a consequence, four different Ba positions are present with coordination spheres

of both the border compounds. The surrounding of the two different apical Al(1X) atoms is thus different: Al(11) resembles the coordination of Al(1) in the 4:5 compound and thus also exhibits longer distance Al(11)–Al(2) (a' : 275.4 pm), whereas Al(12) corresponds to the Al(1) atoms in Ba_3Al_5 and thus shows a slightly decreased Al–Al distance a'' of 272.6 pm.

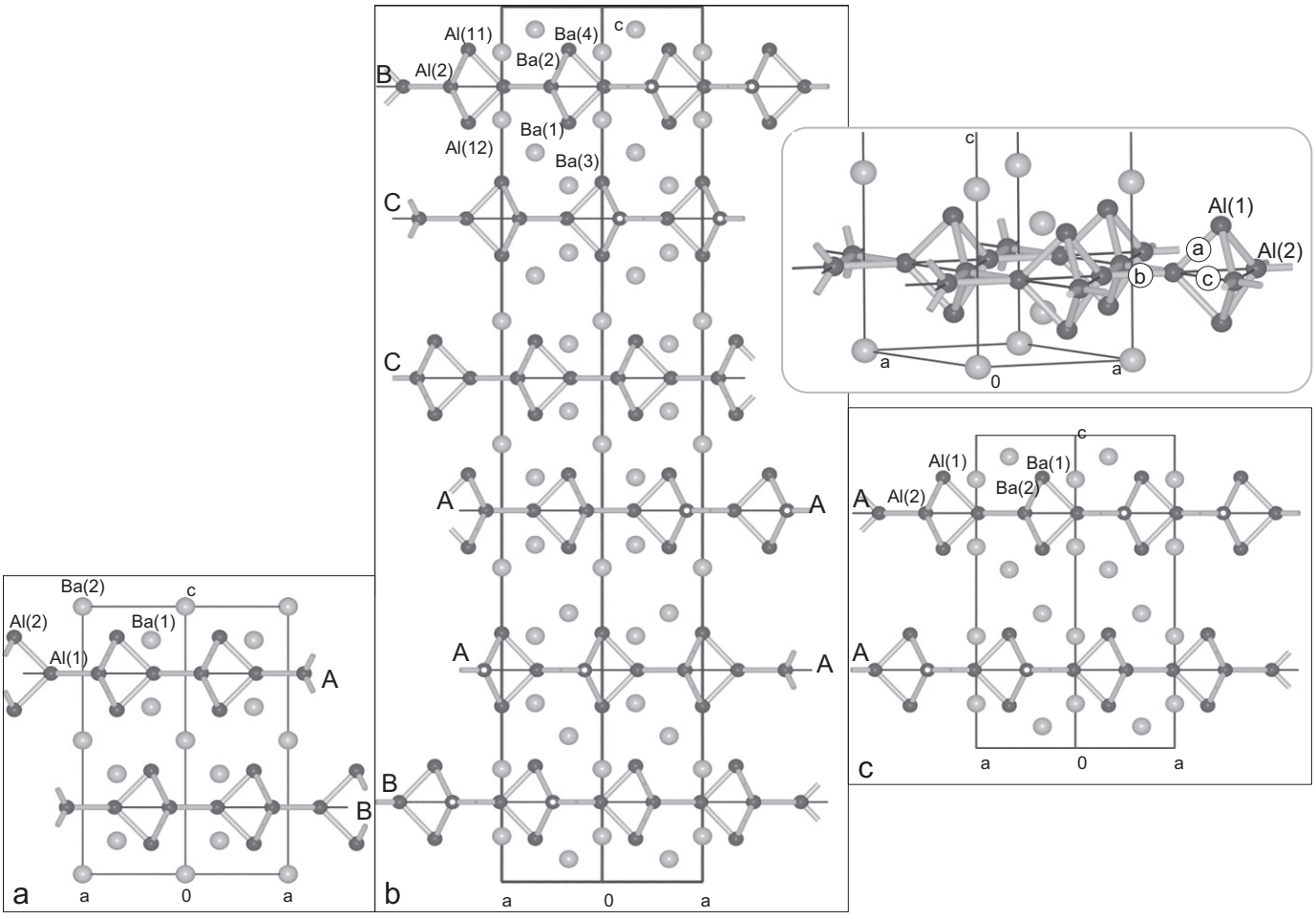

Fig. 1. View of the unit cells of Ba_3Al_5 (a), Ba_7Al_{10} (b) and Ba_4Al_5 (c) in a [110] projection together with a perspective view of one Al_5 layer (grey box top left). (Large light grey spheres: Ba; small dark spheres Al [19].)

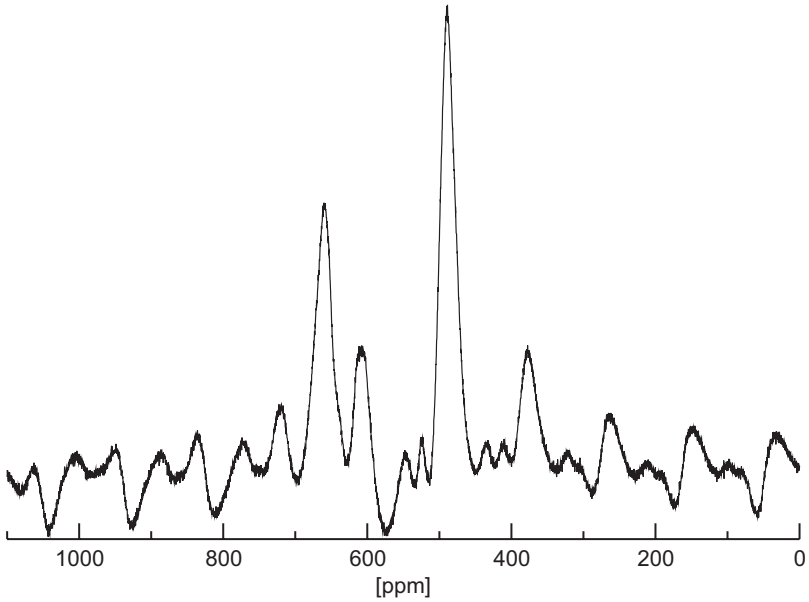

Fig. 2. ^{27}Al-MAS-NMR spectrum of a mixture of Ba_3Al_5 and Ba_7Al_{10} ($B_0 = 11.74$ T; sample spinning rate: 11.5 kHz; 16 000 scans).

3.2. Discussion of the NMR chemical shift

The Al layers in both Ba_4Al_5 and Ba_7Al_{10} contain two chemically different Al positions and consequently the mixture of the two compounds gives rise to two distinct signals in the ^{27}Al MAS-NMR spectra. The integral of the two maxima clearly allows to assign the smaller signal at a chemical shift of 660 pm to the three-bonded Al^{2-} atoms (2×) and the 490 ppm signal to the four-bonded Al^{-} atoms (3×) (Fig. 2). The chemical shift of the four-bonded Al atoms is thus in good agreement with those observed for Al in the clathrates, where the four-bonded Al atoms are also of formal charge −1 and several signals for the crystallographically different Al positions are detected in the range of 280–580 ppm [25]. To our knowledge, reference spectra for a formally Al^{2-} anion isoelectronic to a pentel element have not yet been reported. MAS-NMR spectroscopic measurements of Al_4^{8-} anions in compounds like $Sr_{14}[Al_4]_2[Ge]_3$ are in progress.

3.3. Electronic structure

For the three title compounds, the calculated total density of states (tDOS, above) and the partial DOS (pDOS) of the different Al sites (below) are plotted in Fig. 3 in the range of −8 to +2 eV relative to the *Fermi* level. As expected, the bands in this region are primarily of Al character, with the Al-*s* and -*p* states mostly separated: The *s* bands of the five Al atoms of the structural unit are located between −8 and −2 eV and are grouped in a 2:4:2:2 pattern, indicating equal amounts of strong bonding and antibonding and no net bonding contribution. Significant contributions of $p_{x/y}$-Al(2) (near −5 eV), $p_{x/y}$-Al(1) (−4 to −3.5 eV) and p_z-Al(1) (−2.5 to −3 eV) states are also present in the upper region of this energy range indicating a considerable *sp*-mixing of the Al states. The valence band region between −2 eV and the *Fermi* level is dominated by a complicated overlap of Al-*p* bonding bands which is nevertheless comparable in all three compounds.

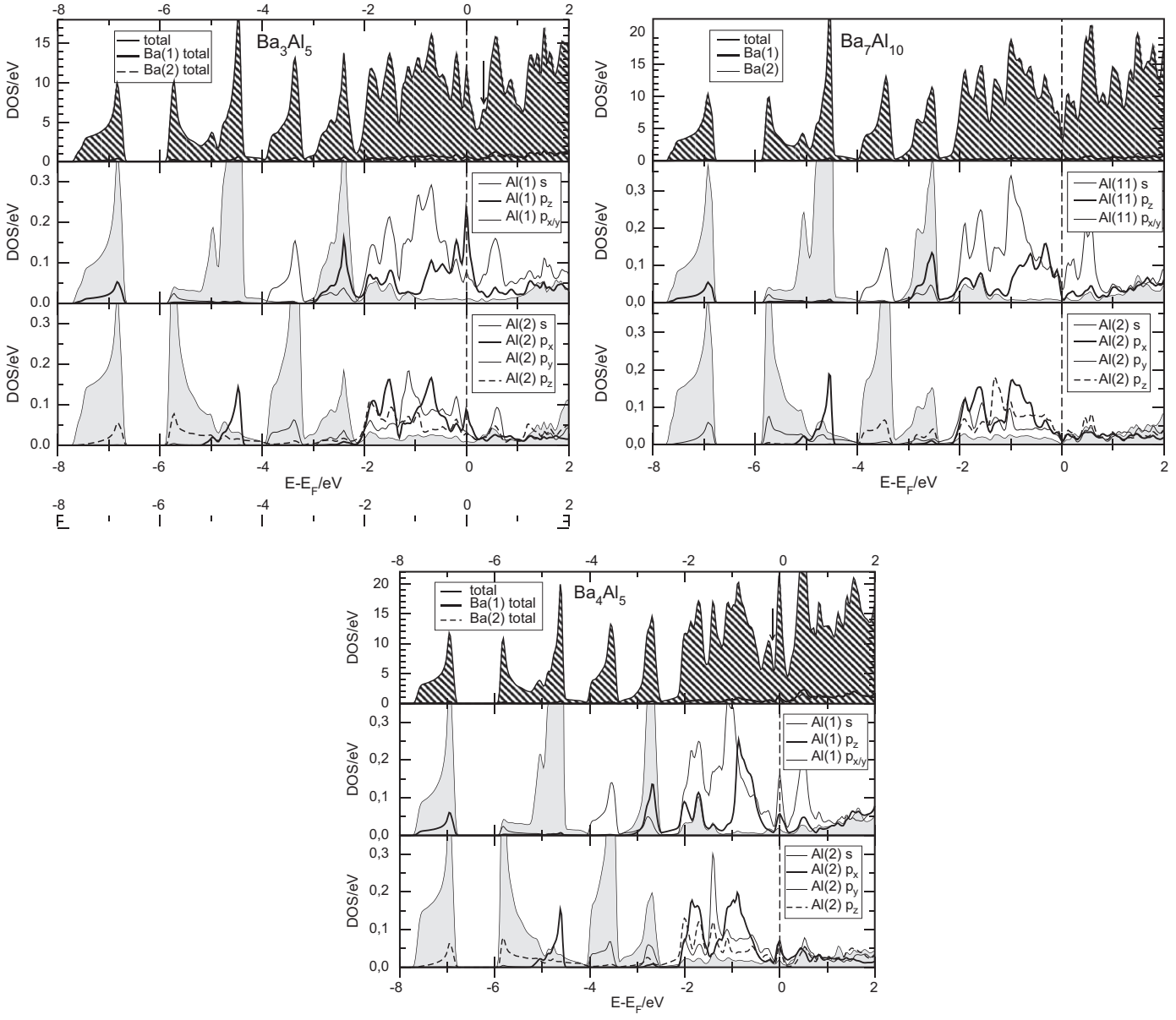

Fig. 3. Calculated total density of states (tDOS) and Ba pDOS (above) together with (below) partial Al states (pDOS) of Ba_3Al_5 (a), Ba_7Al_{10} (b) and Ba_4Al_5 (c) in the range between −8 and 2 eV relative to E_F (shaded curves: Al-*s* states).

Only the new intermediate compound $Ba_{3.5}Al_5$ can be seen as an electron precise *Zintl* compound when ignoring the longer Al(2)–Al(2) contact (distance *c*) of the three-membered rings of the Kagomé nets. In accordance, the calculated electron density map shows no bond critical point at the longer Al–Al contact *c*. Also in agreement with the validity of the *Zintl* electron count, only $Ba_{3.5}Al_5$ shows a pseudo-band gap at the *Fermi* level. This is in full accordance with a simple Hückel calculation reported in [26], where—due to the type of calculation—a real small band gap is observed for Al_5^{7-}. For Ba_3Al_5 the minimum of the tDOS is located above the *Fermi* level, the arrow in Fig. 3 indicates the electron number in the *Zintl* phase and corresponds approximately to the minimum in the tDOS. On the other hand, the ideal number of electrons is situated below the *Fermi* level in the Ba-rich compounds Ba_4Al_5 (see arrow in Fig. 3).

The *Bader* charges (AIM [20]) of the crystallographically different Al atoms meet one's expectation: the Al(1) atoms of formally twofold negative charge exhibit significantly more negative values (−0.72 to −0.92) compared to the formally singly negative Al(2) atoms (charges −0.39 to −0.45). Overall, the charge of the polyanion increases with the Ba content of the compound and the electron transfer from the Ba cations toward the polyanions is comparable for the three compounds (very similar charges for the Ba atoms in all aluminides).

Considering the changes in the population of the Al state with the electron count, it is apparent from the calculation for $Ba_{3.5}Al_5$, and in similar tendency also for the neighbour compounds with lower and higher electron count, that a reduction of the number of electrons—relative to the *Zintl* compound—leads to a depopulation of those Al(1)-p_z states that show predominantly non-bonding character. An increase in the electron count on the other hand leads to a population of the Al $p_{x/y}$ bands. As the latter are mainly anti-bonding in nature, this effect is readily observable in the lengthening of all three Al–Al bonds. The changes on going from Ba_3Al_5 to the electron-precise phase $Ba_{3.5}Al_5$ are less uniform: the large Al–Al distance *c* decreases by a small fraction, the angle at the apical Al becomes more acute and the length of the bond *b* in the smaller three-membered rings of the Kagomé net increases.

Such small changes in binding characteristics of the polyanions upon small changes in their electron counts are not completely without precedent among polar alkaline earth intermetallics with elements at the *Zintl* border, especially the trielides. As a case in point, the isotypic pair Sr_3In_5 [27] and Sr_3In_4Pb [11] demonstrate on one hand that trielides with small deviations from the *Zintl* rules are still stable, and on the other hand that electronic variations within the expected range for electron precise *Zintl* phases are tolerated without a distinct structural change.

References

[1] G. Bruzzone, Boll. Sci. Fac. Chim. Ind. Bologna 24 (1966) 113.
[2] M. Wendorff, C. Röhr, Z. Anorg. Allg. Chem. 631 (2005) 338.
[3] W. Harms, M. Wendorff, C. Röhr, Z. Naturforsch. 62b (2007) 177.
[4] H. Nowotny, A. Mohrheim, Z. Kristallogr. 100 (1939) 540.
[5] M.L. Fornasini, Acta Crystallogr. C44 (1975) 1355.
[6] M.L. Fornasini, Acta Crystallogr. B31 (1975) 2551.
[7] M.L. Fornasini, G. Bruzzone, J. Less-Common Met. 40 (1975) 335.
[8] S. Amerioun, T. Yokosawa, S. Lidin, U. Häussermann, Inorg. Chem. 43 (2004) 4751.
[9] N.B. Manyako, O.S. Zarechnyuk, T.I. Yanson, Kristallografiya 32 (1987) 339.
[10] M. Wendorff, C. Röhr, Z. Anorg. Allg. Chem. 632 (2006) 2164.
[11] M. Rhode, M. Wendorff, C. Röhr, Z. Anorg. Allg. Chem. 632 (2006) 1195.
[12] G.M. Sheldrick, SHELXL-97—Program for the Refinement of Crystal Structures, University of Göttingen, 1997.
[13] M. Wendorff, C. Röhr, Z. Naturforsch., in preparation.
[14] G.M. Sheldrick, SHELXS-97—Program for the Solution of Crystal Structures, University of Göttingen, 1997.
[15] Further details on the crystal structure investigations are available from the Fachinformationszentrum Karlsruhe, Gesellschaft für wissenschaftlich-technische Information mbH, D-76344 Eggenstein-Leopoldshafen 2 on quoting the depository numbers CSD 420090 (Ba_3Al_5), 420091 (Ba_4Al_5), 420092 (Ba_7Al_{10}), the names of the authors, and citation of the paper (E-mail: crysdata@fiz-karlsruhe.de).
[16] P. Blaha, K. Schwarz, G.K.H. Madsen, D. Kvasnicka, J. Luitz, WIEN2K—An Augmented Plane Wave and Local Orbital Program for Calculating Crystal Properties TU Wien, ISBN3-9501031-1-2, 2006.
[17] J.P. Perdew, S. Burke, M. Ernzerhof, Phys. Rev. Lett. 77 (1996) 3865.
[18] A. Kokalj, J. Mol. Graphics Modelling 17 (1999) 176.
[19] L.W. Finger, M. Kroeker, B.H. Toby, J. Appl. Crystallogr. 40 (2007) 188.
[20] R.W.F. Bader, Atoms in Molecules. A Quantum Theory International Series of Monographs on Chemistry, Clarendon Press, Oxford, 1994.
[21] G. Cordier, E. Czech, H. Schäfer, Z. Naturforsch. 37b (1982) 1442.
[22] S. Kal, E. Stoyanov, J.-P. Belieres, T.L. Groy, R. Norrestam, U. Häussermann, J. Solid State Chem. 181 (2008) 3016.
[23] M. Wendorff, C. Röhr, Z. Naturforsch. 62b (2007) 1227.
[24] G. Nargorsen, H. Posch, H. Schäfer, A. Weiss, Z. Naturforsch. 24b (1969) 1191.
[25] C.L. Condron, S.M. Kauzlarich, T. Ikeda, G.J. Snyder, F. Haarmann, P. Jeglic, Inorg. Chem. 47 (2008) 8204.
[26] G.J. Miller, in: S.M. Kauzlarich (Ed.), Chemistry, Structure, and Bonding of Zintl Phases and Ions, VCH Verlagsgesellschaft mbH, Weinheim, 1996.
[27] D.-K. Seo, J.D. Corbett, J. Am. Chem. Soc. 123 (2001) 4512.